Molecular mechanisms of sperm motility are conserved in an early-branching metazoan

Kelsey F. Speer[a], Luella Allen-Waller[a], Dana R. Novikov[a], and Katie L. Barott[a,1]

[a]Department of Biology, University of Pennsylvania, Philadelphia, PA 19104

Edited by John R. Pringle, Stanford University School of Medicine, Stanford, CA, and approved October 19, 2021 (received for review May 28, 2021)

Efficient and targeted sperm motility is essential for animal reproductive success. Sperm from mammals and echinoderms utilize a highly conserved signaling mechanism in which sperm motility is stimulated by pH-dependent activation of the cAMP-producing enzyme soluble adenylyl cyclase (sAC). However, the presence of this pathway in early-branching metazoans has remained unexplored. Here, we found that elevating cytoplasmic pH induced a rapid burst of cAMP signaling and triggered the onset of motility in sperm from the reef-building coral *Montipora capitata* in a sAC-dependent manner. Expression of sAC in the mitochondrial-rich midpiece and flagellum of coral sperm support a dual role for this molecular pH sensor in regulating mitochondrial respiration and flagellar beating and thus motility. In addition, we found that additional members of the homologous signaling pathway described in echinoderms, both upstream and downstream of sAC, are expressed in coral sperm. These include the Na^+/H^+ exchanger SLC9C1, protein kinase A, and the CatSper Ca^{2+} channel conserved even in mammalian sperm. Indeed, the onset of motility corresponded with increased protein kinase A activity. Our discovery of this pathway in an early-branching metazoan species highlights the ancient origin of the pH-sAC-cAMP signaling node in sperm physiology and suggests that it may be present in many other marine invertebrate taxa for which sperm motility mechanisms remain unexplored. These results emphasize the need to better understand the role of pH-dependent signaling in the reproductive success of marine animals, particularly as climate change stressors continue to alter the physiology of corals and other marine invertebrates.

coral | soluble adenylyl cyclase | pH | reproduction | cyclic AMP

The activation of sperm motility requires precise temporal and spatial control in order to maximize chances of egg–sperm contact and fertilization (1). Despite the vital importance of this process for reproductive success across metazoan phyla, the molecular mechanisms that regulate sperm activation remain poorly understood. Sperm are typically held in an inactive state within the male prior to release into either the surrounding water column during broadcast spawning, as in early-branching metazoans and many bilaterians, or directly into the female oviduct during copulation, as in some bilaterians (2). The signals that trigger sperm motility following release vary between environments and species and can include changes in osmolarity, ion concentrations (e.g., bicarbonate), and/or chemical signals released by eggs (3). Even with the considerable differences in reproductive ecology and activation cues that characterize different taxa, the downstream signaling pathways that activate motility are highly conserved across the few taxa that have been described to date, namely mammals (phylum Chordata) and sea urchins (phylum Echinodermata). Because of the historical focus on these two phyla, which are closely related in the context of metazoan evolution, we know very little about the broader evolution of the molecular pathways that activate sperm motility across the metazoan phylogeny and especially in earlier branching metazoan phyla. This has left a significant gap in our understanding of the evolution of the mechanisms that regulate sperm function, an important issue to address given the importance of these mechanisms for determining animal fitness in a changing environment.

Reef-building corals, members of the early-branching phylum Cnidaria, are an evolutionarily and ecologically important model system for understanding mechanisms of sperm motility. First, corals belong to one of the earliest phyla to evolve organized tissues, and as diploblasts, they lack the mesoderm present in bilaterians (4). Second, corals are the foundational species of coral reefs, one of the most biodiverse ecosystems on the planet (5). Coral reproduction is essential for the persistence of reefs worldwide (6) and in most species involves the tightly coordinated release of sperm and eggs into the water column on just a few nights each year (7, 8). This process is currently threatened by a combination of local stressors (9) and global climate change (10–12). Sperm in particular are acutely susceptible to environmental disturbances due to their small size and brief lifespan (13), and climate change stressors including ocean warming and acidification have reduced coral sperm production (11, 14), motility (10, 15, 16), and fertilization success (17, 18) in several species. The mechanisms driving these declines in sperm performance are unknown, but both warming and acidification may disrupt coral cellular metabolism and acidify the cytosol (19–21), two processes that are important for sperm motility in other species (22). Indeed, initial evidence indicates that alkalinization of coral sperm cytosol promotes motility (23), highlighting the importance of understanding the

Significance

Reef-building corals are the keystone species of the world's most biodiverse yet threatened marine ecosystems. Coral reproduction, critical for reef resilience, requires that coral sperm swim through the water column to reach the egg. However, little is known about the mechanisms that regulate coral sperm motility. We found here that coral sperm motility is pH dependent and that activation of motility requires signaling via the pH-sensing enzyme soluble adenylyl cyclase. This study reveals the deep conservation of a sperm activation pathway from humans to corals, presenting the first comprehensive examination of the molecular mechanisms regulating sperm motility in an early-diverging animal. These results are critical for understanding the resilience of this sensitive life stage to a changing marine environment.

Author contributions: K.F.S. and K.L.B. designed research; K.F.S., L.A.-W., D.R.N., and K.L.B. performed research; K.F.S., L.A.-W., D.R.N., and K.L.B. analyzed data; and K.F.S., L.A.-W., and K.L.B. wrote the paper.

The authors declare no competing interest.

This article is a PNAS Direct Submission.

[1]To whom correspondence may be addressed. Email: kbarott@sas.upenn.edu.

This article contains supporting information online at http://www.pnas.org/lookup/suppl/doi:10.1073/pnas.2109993118/-/DCSupplemental.

Published November 22, 2021.

molecular pathways that connect pH-dependent signaling with changes in cellular performance.

Alkalinization of the sperm cytosol acts as a critical intracellular messenger controlling the onset of motility in several species (3, 24, 25). In sea urchins, the binding of egg-derived peptides [e.g., speract (2)] to guanylyl cyclase (GC) receptors at the cell surface activates a sperm-specific Na^+/H^+ exchanger [SLC9C1 (26)], which increases cytoplasmic pH through its proton efflux activity. In both spawning marine invertebrates and mammals, this alkalinization stimulates cAMP production via the enzyme soluble adenylyl cyclase [sAC (27)], leading to protein kinase A (PKA)-dependent phosphorylation of flagellar proteins and calcium signaling via CatSper channels (2), which together stimulate flagellar beating. Cnidarian GC-A receptors and CatSper channels are highly conserved with those from sea urchins (28, 29), and although the other constituents of the pathway have yet to be investigated, these reports suggest that this molecular mechanism may be conserved in early-branching metazoans. Mammals have evolved a distinct activation signal that nonetheless utilizes a similar signaling cascade to that of sea urchins, whereby elevated levels of bicarbonate in the female reproductive tract activate sAC (30), and the resulting burst of cAMP activates PKA, leading to phosphorylation of flagellar proteins and ultimately motility. Each component of this conserved pathway appears to be necessary for sperm motility and fertilization in mammals, as mice lacking SLC9C1, sAC, PKA, or CatSper display severe sperm motility defects, rendering them infertile (31–35). These studies support the conservation of sAC-cAMP as a central signaling node in sperm activation across bilateria; however, there is no data currently on the role of sAC-cAMP signaling in early-branching metazoans. In corals, somatic tissues express a functional homolog of sAC that is stimulated by bicarbonate to make cAMP (36), and this enzyme plays a role in responding to pH fluctuations within the cell (37), leaving open the promising possibility that this pathway is functionally conserved in coral sperm.

In order to test the hypothesis that sperm motility in early-branching metazoans is regulated by a molecular signaling pathway that is conserved with bilaterians, we examined the role of intracellular pH, sAC, cAMP, and PKA signaling in sperm motility in the reef-building coral *Montipora capitata* using a combination of microscopy, biochemistry, and immunological assays. In addition, we analyzed the expression and conservation of key proteins in the echinoderm motility initiation pathway in *M. capitata* sperm via interrogation of RNA sequencing (RNA-seq) databases and in silico structural analyses. This comprehensive examination of the intracellular signaling pathways that regulate sperm motility in an early-branching metazoan highlights the functional conservation of a fundamental pathway essential for animal reproduction. Furthermore, the mechanisms underlying coral sperm motility have important implications for determining how climate change will influence the reproductive success of corals and other marine animals.

Results

Response of Coral Sperm to Cytosolic Alkalinization. To induce cytosolic alkalinization, sperm from the coral *Montipora capitata* were suspended in sodium-free seawater (NaFSW) and exposed to 20 mM NH_4Cl (23, 38, 39). Intracellular pH (pH_i) and motility were then monitored simultaneously by confocal microscopy using the fluorescent dye SNARF-1-AM (*SI Appendix*, Fig. S1). Prior to NH_4Cl treatment, sperm were inactive (0% motility) and had a mean pH_i of 7.52 ± 0.05 (Fig. 1*A*). Sperm pH_i increased following NH_4Cl exposure, reaching a peak of 8.31 ± 0.04 within 45 s (Fig. 1*A*), equivalent to over an 80% decrease in H^+ concentration. Sperm pH_i remained above pH 8.0 for at least 2:30 min and then started to decline after 3:00 min, reaching initial levels after 4:30 min and continuing to decline over the next 2:00 min, reaching a minimum of pH 7.26 ± 0.02 (Fig. 1*A*). Motility increased instantaneously following exposure to NH_4Cl (visual observation), reaching

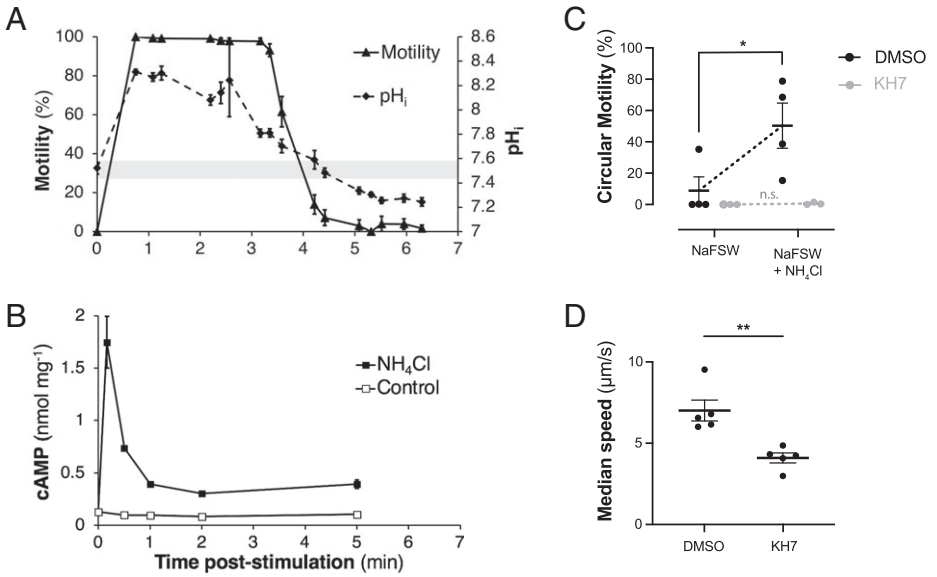

Fig. 1. Response of sperm from the coral *Montipora capitata* to ammonium chloride (NH_4Cl) treatment and sAC inhibition. (*A*) Coral sperm motility (solid line) and pH_i (dashed line) after exposure of sperm in NaFSW to 20 mM NH_4Cl ($n \geq 15$ cells per time point). Gray shaded region indicates 99% CI of sperm initial pH_i prior to activation (7.52 ± 0.05). (*B*) Concentration of cAMP in coral sperm in NaFSW following treatment with 20 mM NH_4Cl (black squares) or control (open squares). cAMP levels are normalized to total protein. (*C*) Circular motility of coral sperm in NaFSW preincubated with 0.2% DMSO (black) or 50 µM sAC inhibitor KH7 (gray) before and after treatment with NH_4Cl. The horizontal black bar represents the mean of $n \geq 3$ replicates. (*D*) The median speed of coral sperm in seawater pretreated with 0.2% DMSO or 50 µM KH7. The horizontal black bar represents the mean of $n = 5$ replicates. Error bars in *A*, *C*, and *D* indicate SEM; error bars in *B* indicate SD; where not visible, they fall within the symbol. Significance is denoted as n.s. (no significance), $*P \leq 0.05$, $**P \leq 0.01$.

100% within 45 s postexposure (Fig. 1*A*). Motility remained near 100% for 3:20 min and then rapidly decreased to 7.1% after 4:25 min and remained near zero until the end of the experiment (Fig. 1*A*). This drop in motility was concurrent with declining pH_i, with a possible motility threshold of pH_i ~7.8. Treatment of sperm with 20 mM NH_4Cl also led to a rapid increase in cAMP content within 15 s followed by a decline by ~60 s postexposure (Fig. 1*B*). Interestingly, the absolute concentration of cAMP produced by sperm varied between spawning seasons, with a peak of 1.7 ± 0.017 nmol · mg^{-1} occurring in 2019 (Fig. 1*B*) and peaks between 45 to 96 pmol · mg^{-1} in 2021 (*SI Appendix*, Fig. S2). Sperm cAMP concentrations remained two- to threefold higher than initial levels for up to 5 min postexposure, while unexcited control sperm exhibited little change in cAMP content (Fig. 1*B* and *SI Appendix*, Fig. S2).

In order to determine if sAC was necessary for NH_4Cl-stimulated sperm motility, sperm were incubated with the sAC-specific inhibitor KH7 or a dimethyl sulfoxide (DMSO) carrier control prior to NH_4Cl treatment. In the DMSO pretreatment, addition of NH_4Cl led to a significant increase in the percentage of cells exhibiting circular motility, from 8.9 ± 17.6% prestimulation (Video S1) to 50.3 ± 28.9% poststimulation (P = 0.0423, Tukey's posthoc test; Video S2 and Fig. 1*C*). In contrast, pretreatment with 50 μM KH7 abolished the activation of circular motility following NH_4Cl treatment, which remained <1% (Fig. 1*C* and Video S3). The flagella of KH7-treated cells remained structurally intact, displaying a weak beating motion near the head that did not propagate along the length of the flagellum (Video S4). KH7 treatment also caused a significant decrease in the median speed of coral sperm maintained in seawater, from 7.0 ± 1.3 to 4.1 ± 0.6 μm · s^{-1} (P = 0.0079, Wilcoxon test; Fig. 1*D*).

Expression of sAC in Coral Sperm. The sequence of *M. capitata* sAC (*mc*sAC) was identified by querying an *M. capitata* sperm genome (40) using a complementary DNA (cDNA) sequence from the coral *Pocillopora damicornis* [*pd*sAC (37)]. The predicted protein was 75.7% similar to *pd*sAC and 48.3% similar to sAC from the sea urchin *Strongylocentrotus purpuratus* (*sp*sAC; *SI Appendix*, Table S1). Sequence alignment with metazoan homologs (*SI Appendix*, Table S2) revealed that *mc*sAC contained both conserved cyclase homology domains (CHD1 & CHD2; *SI Appendix*, Fig. S3) necessary for bicarbonate-stimulated cAMP production (41). Within its catalytic core, *mc*sAC shared six of seven active site residues with *M. musculus* sAC (42) and seven of seven with cnidarian (*pd*sAC) and echinoderm sAC (*sp*sAC; *SI Appendix*, Fig. S3). *mc*sAC activity was detected in crude *M. capitata* sperm lysates as evidenced by a dose-dependent activation of AC activity in response to 0–5 mM Mn^{2+} (*SI Appendix*, Fig. S4), a cofactor that activates sAC but not related transmembrane ACs [tmACs (43)]. Like *pd*sAC, *mc*sAC lacked the short autoinhibitory peptide directly C-terminal to CHD2 (*SI Appendix*, Fig. S3) that has been described in mammals (44). *mc*sAC also contained a long (~140 kDa) C-tail of unknown function, which has been found in all metazoan sAC genes.

Expression of *mc*sAC in sperm was confirmed by Western blot using anti-coral sAC antibodies recognizing CHD2. The predominant isoform was the full-length protein (~195 kDa, sAC_{FL}; Fig. 2*A*) followed by an ~110-kDa isoform (sAC_{110}; Fig. 2*A*) and two additional isoforms of ~55 and 45 kDa (sAC_{55} and sAC_{45}, respectively) which were detected at low levels (Fig. 2 *A*, *Right*). sAC_{55} and sAC_{45} are similar in size to two truncated forms of sAC identified in mammalian somatic tissues, including a highly active form composed of only CHD1 and 2 [sAC_T; ~55 kD (41)] and possibly an atypical variant of sAC lacking CHD1 [~46 kDa (45)]. Expression of sAC_{FL} was not detected in adult *M. capitata* tissues, which only expressed the smallest ~45-kDa isoform at detectable levels (Fig. 2*B*). Running as a doublet, these bands may represent posttranslational modifications of sAC_T.

The subcellular localization of *mc*sAC in sperm was determined by immunocytochemistry using the same anti-coral sAC antibodies. *M. capitata* sperm consist of a head that contains the nucleus and acrosomal compartment and a flagellum with a single 9 + 2 microtubule bundle that includes two distinct regions: the midpiece adjacent to the head that contains five to six mitochondria followed by the principle piece (i.e., tail) containing just the axonemal fibers (Fig. 2*C*) (46). *M. capitata* sperm expressed *mc*sAC throughout the entire cell, and expression was most concentrated in the midpiece (Fig. 2 *D–F*). *mc*sAC was also present in low abundance at the tip of the sperm head in the predicted acrosomal region (Fig. 2 *D–F*) and across the entire length of the flagellum (Fig. 2 *G* and *H*), where it colocalized with β-tubulin, the primary component of the axonemal fibers (Fig. 2 *E* and *F*). Controls confirmed antibody staining was specific for *mc*sAC for both Westerns (*SI Appendix*, Fig. S5 *B* and *D*) and immunostaining (*SI Appendix*, Fig. S6).

Expression of a Conserved Bilaterian Signaling Core in Coral. Next, we next analyzed the expression of key players in the sAC-dependent sperm activation pathway in coral sperm, both those conserved across bilateria (PKA, SLC9C1 [sNHE], and CatSper) and those that have only been described in sea urchins (GC-A, HCN, and CNGK; Fig. 3*A*). We began by searching for each protein sequence in two *M. capitata* genomes (40, 47) using sea urchin homologs to identify reciprocal best BLAST hits (*SI Appendix*, Table S1). *M. capitata* genomic sequences were then used to query a sperm RNA-seq database derived from the same species (48). Further structural analysis was carried out using sequence alignment and transmembrane helix prediction software in order to identify key functional domains (Fig. 3 *B–H* and *SI Appendix*, Tables S2–S4 and Figs. S7–S10). In cases in which the *M. capitata* genome predicted a structurally incomplete protein, a comparison with the well-annotated genome of *P. damicornis* was used to identify potential missing sequences (dotted lines; Fig. 3 *D*, *F*, and *G*). Together, these analyses identified a single homolog of each gene in the *M. capitata* genome and at least nine transcripts of 95% or greater homology to the genomic sequence expressed in the *M. capitata* sperm transcriptome (*SI Appendix*, Table S1).

The catalytic domain of PKA in *M. capitata* sperm was 90.6% similar to *S. purpuratus* PKA Cα, encoding a polypeptide of ~40 kDa (Fig. 3*B* and *SI Appendix*, Table S1). Protein expression of PKA Cα in *M. capitata* sperm was further confirmed by Western blot (Fig. 3*B*). The band ran as a triplet, likely because of activating phosphorylation of the kinase activation loop (49). PKA substrate phosphorylation in sperm activated with 20 mM NH_4Cl was also detected by Western using an antibody that recognized the consensus sequence of the enzyme (RRXS*/T*; Fig. 3*C*). Many proteins ranging in size from ~15 to ~250 kDa exhibited a pattern of increased phosphorylation upon motility stimulation.

The *M. capitata* homolog of SLC9C1 (i.e., sNHE), a sodium/hydrogen exchanger that elevates cytoplasmic pH upstream of sAC and PKA (Fig. 3*A*), was 69.8% similar to SLC9C1 from *S. purpuratus* (*SI Appendix*, Table S1). *mc*SLC9C1 contained an N-terminal sodium–proton exchanger (NHE) domain with the canonical cation-binding motif of 1:1 electroneutral exchangers embedded within the predicted S3-4 region, identical to echinoderms but distinct from mammals (Fig. 3*D* and *SI Appendix*, Fig. S7*A*). C-terminal to the NHE, *mc*SLC9C1 also had both a voltage-sensing domain (VSD) and a cyclic nucleotide-binding domain (CNBD; Fig. 3*D*). The *mc*SLC9C1 VSD displayed the

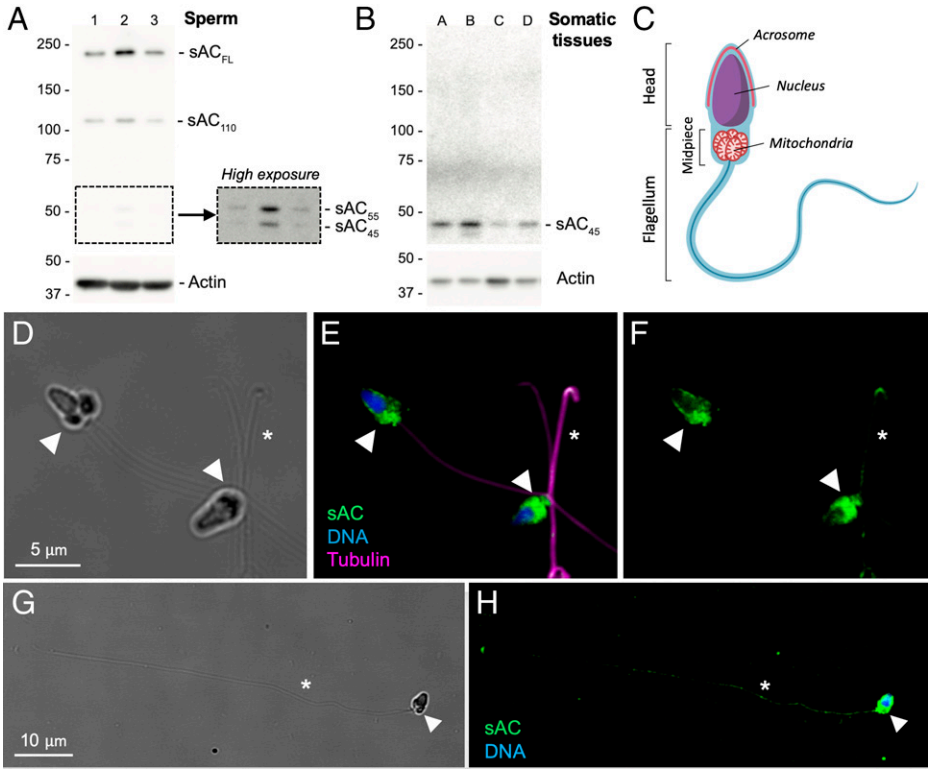

Fig. 2. Expression of sAC in *Montipora capitata* sperm. (*A*) Western blot of the sAC protein in sperm from three different individuals (lanes 1 to 3) shows high expression of two isoforms (sAC_{FL}, sAC_{110}) and low expression of two isoforms (sAC_{55}, sAC_{45}). (*Inset*) High exposure of same blot. Approximate size (kDa) of each protein is indicated on the left. (*B*) Western blot of somatic tissues from four *M. capitata* adults (lanes A to D) show expression of a single sAC isoform (sAC_{45}). (*C*) Diagram of the architecture of coral sperm, identified by ref. 46. The head houses the nuclei and the surrounding acrosome compartment. The flagellum contains the axoneme formed from a 9 + 2 microtubule bundle and, immediately posterior to the head, a mitochondria-rich midpiece. (*D*) Brightfield image of sperm. (*E*) Corresponding fluorescence micrograph showing localization of sAC (green), DNA (blue), and flagella (magenta; stained with anti-β-tubulin antibodies). (*F*) Corresponding image of coral sAC expression alone. (*G*) Brightfield image of a sperm cell with the flagellum extended. (*H*) Corresponding fluorescence micrograph highlighting coral sAC expression along the length of the flagellum. Arrowheads indicate the midpiece of the flagellum containing the mitochondrial sheath, and asterisks indicate the flagellum.

four-transmembrane (S1-4) architecture, including the seven positively charged residues in S4 found in the *Drosophila* Shaker channel (*SI Appendix*, Fig. S7*B*) (50). While these charged residues are entirely conserved in echinoderms, they are only semiconserved in mammals, reflecting the divergence of the pathway from its invertebrate ancestors.

The four polypeptides that assemble to form the pore of the CatSper calcium ion channel [CatSper1-4α (51)] were identified in *M. capitata* sperm and shared up to 70.7% similarity with their *S. purpuratus* homologs but were 27.7 to 74.3% shorter, likely due to incomplete genome coverage (*SI Appendix*, Table S1 and Fig. S8*A*). When the partial sequences were overlaid, a consensus of the classic 6TM-type architecture common to CatSpers emerged (Fig. 3*E*). For example, *mc*CatSper2-4α each contained a VSD with four to five charged amino acids in transmembrane segment S4 as compared with the six to seven found in the sea urchin *S. purpuratus* and the two to four found in *M. musculus* (*SI Appendix*, Fig. S8*B*). In *mc*CatSper1, 2, and 4α, segments S5 and S6 were linked by a short interconnecting helix, or "selectivity filter," with the canonical [T/S]x[D/E]xW motif of Ca^{2+}-selective channels (Fig. 3*E* and *SI Appendix*, Fig. S8*C*). *mc*CatSpers 2 and 3α contained short, cytoplasmic domains C-terminal to S6 that were predicted to form coiled-coil domains, important for subunit oligomerization in mammals (*SI Appendix*, Table S4 and Fig. S8*A*) (51, 52). Transcripts of CatSper2-4α were identified in *M. capitata* sperm (*SI Appendix*, Table S1), and while *mc*CatSper1α was not found, it is notable that the stable expression of the four bilaterian subunits is highly interdependent (53). Thus, the absence of *mc*CatSper1α is likely due to an inability to identify the C terminus of the protein via homology searches of the genome, which, combined with the inherent 3' bias of the poly-A selection method used to generate the RNA-seq library (48), likely obscured actual expression data.

Considering specific members of the sea urchin pathway (Fig. 3*A*), the *M. capitata* guanylyl cyclase receptor (mcGC-A) gene was 42.3% similar to *S. purpuratus* GC-A (synonymous with the Speract receptor) and 78.0% similar to that of the coral *Euphyllia ancora* (eaGC-A; *SI Appendix*, Table S1). *mc*GC-A contained an intracellular kinase-like homology (KL) domain and a guanylyl cyclase catalytic domain (CY) as well as an extracellular ligand-binding domain (LB; Fig. 3*F*), similar to both the Speract receptor and *ea*GC-A. Sea urchin sperm activation via GC-A also involves the ion channels CNGK and HCN. CNGK-dependent membrane hyperpolarization activates SLC9C1 to induce cytosolic alkalinization, whereas HCN-dependent membrane depolarization occurs downstream of sAC to facilitate CatSper activation (Fig. 3*A*) (2). Like CatSper, both CNGK and HCN assemble as a tetramer of 6TM-type subunits, however, with a C-terminal CNBD replacing the CatSper coiled-coil domain (Fig. 3 *G* and *H*, respectively). *mc*CNGK was 53.9% similar to CNGK characterized in the sea urchin *Arabica punctulata* (*SI Appendix*, Table S1), and its four subunits were encoded as domains within a single polypeptide (Fig. 3*G*). In contrast, HCN channels form from a homotetramer (54), and the single 6TM repeat of *mc*HCN (Fig. 3*H*)

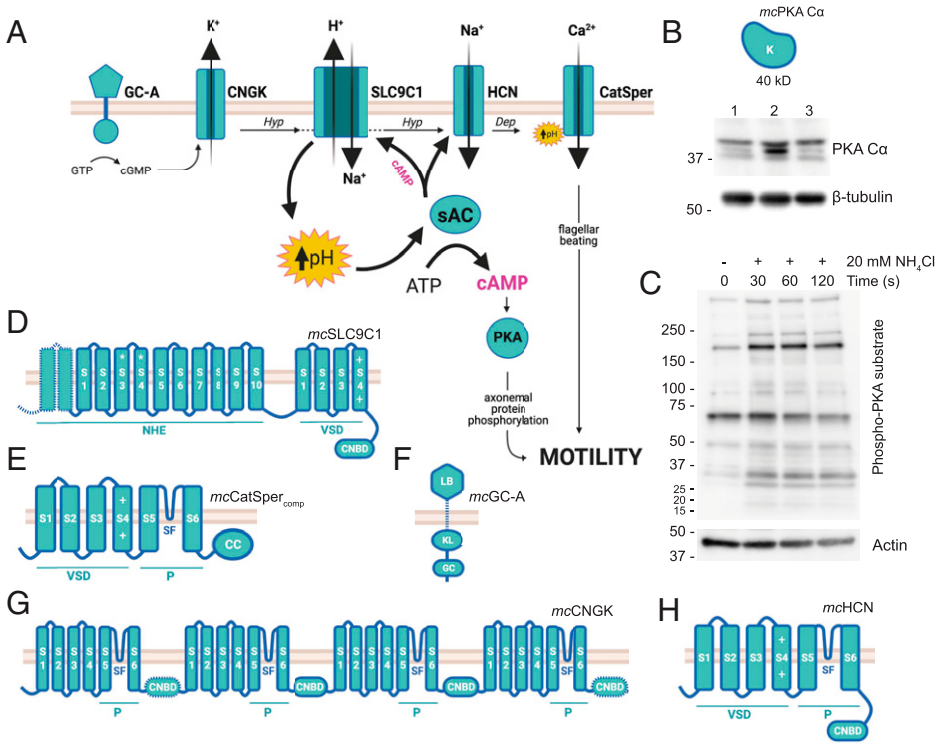

Fig. 3. A pH-dependent motility pathway is conserved in sperm from the coral *Montipora capitata*. (*A*) Diagram of the pH-sAC-cAMP motility pathway from echinoderms. Egg-derived chemoattractants bind to a guanylyl cyclase receptor (GC-A) which produces cGMP to stimulate CNGK-mediated K^+ efflux and membrane hyperpolarization (Hyp). CNGK activates the H^+/Na^+ exchanger SLC9C1, which raises cytoplasmic pH, thereby activating sAC-dependent cAMP production and driving PKA-dependent phosphorylation of axonemal proteins controlling motility. sAC-dependent cAMP feeds back to maintain SLC9C1 activity and promotes hyperpolarization-dependent activation of HCN, which depolarizes (Dep) the cell via Na^+ influx. The CatSper channel responds to both depolarization and elevated pH to generate Ca^{2+} influx signals that alter the flagellar waveform. (*B*) Expression of a predicted 40-kDa *M. capitata* PKA Cα catalytic subunit was confirmed by Western blot. The protein ran as a triplet, likely because of activating phosphorylations. (*C*) Western blot analysis also detected an increase in PKA substrate phosphorylation in sperm stimulated with 20 mM NH_4Cl. Predicted domain structures of *M. capitata* homologs of (*D*) *mc*SLC9C1, (*E*) *mc*CatSper$_{comp}$, (*F*) *mc*GC-A, (*G*) *mc*CNGK, and (*H*) *mc*HCN. Conserved protein domains and amino acid signatures: K, kinase domain; S, transmembrane segment; NHE, sodium hydrogen exchange domain; *, includes NHE consensus sequence; VSD, voltage sensing domain; +, positively charged amino acids involved in voltage sensing; CNBD, cyclic nucleotide-binding domain; P, pore-forming domain; SF, selectivity filter; CC, coiled-coil domain; GC, guanylyl cyclase domain; KL, kinase-like domain; LB, ligand-binding domain.

was 73.1% similar to the *S. purpuratus* homolog (*sp*HCN;*SI Appendix*, Table S1). Like their echinoderm homologs, the selectivity filters of both *mc*CNGK and *mc*HCN contained a canonical cation-binding GYG motif of cation channels (*SI Appendix*, Figs. S9 and S10*A*). This region in *mc*HCN was nearly identical to *sp*HCN (100% similarity; *SI Appendix*, Fig. S10*A*), a channel whose weak selectivity for K^+ [P_K/P_{Na} = 4.7 (55)] causes a depolarizing inward Na^+ current under physiological conditions (56). In contrast, the T/S-rich region in the *mc*CNGK filter (*SI Appendix*, Fig. S9) is indicative of highly K^+-selective channels (56). Additionally, *mc*HCN transmembrane segment S4 contained eight positively charged amino acids, broken into two clusters of three to four residues, that comprise a predicted VSD (*SI Appendix*, Fig. S10*B*). *mc*CNGK, however, lacked a VSD, suggesting this channel responds solely to cGMP and not to changes in membrane polarization.

Discussion

Cyclic AMP Is a Conserved Signaling Mechanism in Sperm Activation. Here, we demonstrate in an early-branching metazoan that sperm motility is initiated via a pH- and cAMP-dependent signaling pathway. Chemical alkalinization of inactive *Montipora capitata* sperm was sufficient to induce 100% motility. A subsequent reacidification of the cytosol began ~2.5 min after alkalinization, with pH_i eventually passing below the initial setpoint. This overcompensation is consistent with the presence of active acid–base compensatory mechanisms in coral sperm. In addition, once pH_i declined below pH 7.8, sperm motility also began to decline, indicating that coral sperm may have a threshold for motility around pH_i 7.8, similar to echinoderm sperm (24). While the mechanistic link between declining pH_i and reduced coral sperm motility remains uncharacterized, data from other marine invertebrate models suggest that the dynein ATPase, the key motor protein driving flagellar beating, is most active when pH_i is ≥ 7.5 and may be directly inhibited by reacidification (22, 57). Cytosolic alkalinization in coral sperm also coincided with rapid cAMP production that peaked within the first 30 s of activation, indicating that this universal second messenger molecule is involved in the onset of coral sperm motility. A similar burst of total cAMP occurs in both mammalian (58) and echinoderm sperm (59) and in those taxa initiates a signaling cascade that up-regulates flagellar beating and alters the flagellar waveform (2). Our data suggest that this pH-dependent cAMP signaling is not unique to bilaterian sperm but instead arose before the split of the cnidarian and bilaterian lineages.

sAC Plays a Central Role in Coral Sperm Physiology. The molecular pH sensor sAC is the primary source of cAMP driving the onset of sperm motility in bilaterians and it plays a central role in the regulation of sperm physiology (30, 60). We found here that sAC is expressed and active in coral sperm and is required for the onset of coral sperm motility in response to pH. Thus, our data extend the conservation of the sAC signaling node in

sperm prior to divergence with bilaterians. While the role of tmAC in coral sperm cAMP production cannot be ruled out, these enzymes are insensitive to pH and bicarbonate and do not play a major role in flagellar motility in bilaterian sperm (27, 61, 62). In contrast, sAC is activated in response to local fluctuations in sperm cytoplasmic pH in both mammals (63) and echinoderms (64), and our data confirm that sAC in corals is both active in sperm and an important regulator of motility.

Coral sperm expressed sAC throughout the head, midpiece, and distal region of the flagellum, indicating that sAC may be involved in multiple aspects of coral sperm physiology. For example, abundant expression along the midpiece, a localization that is conserved in sea urchin (64) and mammalian sperm (30), suggests that coral sAC may influence cellular respiration. Sperm motility and respiration are tightly coupled through the dynein ATPase, which consumes the vast majority of cellular ATP (22). Studies of bilaterian somatic cells have uncovered a unique pool of sAC that resides within the mitochondrial matrix and promotes PKA-dependent up-regulation of oxidative phosphorylation (65). Here, we show that the onset of coral sperm motility coincides with an increase in PKA substrate phosphorylation throughout the cell. While the identity of coral PKA substrates remain unknown, many of the PKA targets in sea urchin sperm are mitochondrial proteins (66). It is possible that regulation of mitochondrial output via sAC-PKA signaling in invertebrate sperm is an additional means of "tuning" flagellar motility. Importantly, because mitochondrial function and sperm motility are both impaired under simulated ocean acidification in sea urchin, mussel, and ascidian sperm (21, 67), a description of the molecular mechanisms underlying sperm motility and their response to environmental conditions is critical for predicting the susceptibility of reproduction to climate change.

Localization of coral sAC along the entire length of the flagellum suggests an additional specialized role for this enzyme in motility. sAC also associates closely with the axoneme in sea urchins (64), where the large surface-area-to-volume ratio allows for rapid transmembrane signaling and direct contact with axonemal proteins (68). In addition, the other members of the motility pathway all localize almost exclusively to the sea urchin flagellum, including GC-A and CNGK (69), SLC9C1 (26), HCN (56), and CatSper (70), allowing for tight coupling of this signal transduction pathway. Although it remains to be determined where these proteins are expressed in coral sperm, it is likely that they similarly colocalize with coral sAC along the flagellum. In mouse sperm, sAC is expressed primarily in the midpiece but is not detected by immunocytochemistry in the principal piece (30). However, sAC activity has been observed in both of these compartments in mice, albeit with different kinetics (61), and the molecular mechanisms driving these differences remain to be described. Finally, the expression of coral sAC in the sperm head suggests it may play a role in the acrosome reaction, much like it does in sea urchins (64) and possibly in mammals (60). Interestingly, sea urchin sperm exhibit compartment-specific differences in sAC isoform expression, with sAC_T localizing to the head and sAC_{FL} along the flagellum (64). The functional significance of this partitioning remains unknown but could lead to differences in enzyme kinetics between the head and the flagellum that influence their disparate roles in the acrosome reaction and motility, respectively.

Expression of multiple sAC isoforms due to alternative splicing is common in metazoans (71), and corals are no exception (Fig. 2) (37). Coral sperm expressed multiple isoforms of sAC, including sAC_{FL}. That coral sAC_{FL} expression was restricted to the male germline, as it is in both mammals (30, 41) and echinoderms (64), suggests that there may be a conserved sperm-specific function of this isoform. However, the precise role of sAC_{FL} in cellular physiology remains enigmatic across all species examined to date. Interestingly, the autoinhibitory peptide described in mammalian sAC_{FL} (44) is absent in *mc*sAC and in sAC from all other coral species examined so far, which may contribute to the relatively high AC activity observed in corals (36) and highlights the need to understand more about the role of the sAC C-tail across metazoan species. Coral sperm also expressed several shorter isoforms, including an ~100-kDa sAC isoform and two other small ~45- to 55-kDa isoforms in low abundance. These smallest isoforms were also expressed in somatic coral tissues and may represent sAC_B which is commonly expressed in both germline and somatic cells of bilaterians (41, 64). All together, these data suggest that sAC plays a conserved and complex role as a central regulator of sperm physiology across metazoa, and much work remains to unravel the many potential roles of this enzyme in sperm physiology of corals and other early-branching metazoans.

Conservation of a cAMP-Dependent Motility Pathway across Metazoans. A comprehensive analysis of the molecular mechanisms underlying sperm activation in coral confirmed the expression and high structural conservation of the entire echinoderm sperm activation pathway in an early-branching metazoan. These results indicate that coral sperm activation couples environmental sensing to a cytoplasmic signaling pathway dependent on intracellular alkalinization and the central regulatory node of sAC-cAMP. The ability of sperm to remain in a quiescent state until they detect an egg nearby allows males to optimize their fertilizing capacity by saving their limited energy and increasing their chances of encountering eggs by using directional motility toward the cue (i.e., chemotaxis) (2). The majority of extant spawning marine invertebrates use chemotaxis, including corals, various other cnidarians, molluscs, echinoderms, and ascidians (72), and this capacity is critical for fertilization (Fig. 4). In each of these lineages, we find functional data supporting the conservation of the pH-sAC-cAMP pathway (Fig. 4) (2, 73). Genetic evidence for the coevolution of sAC, SLC9C1, and CatSper also links this pathway to even earlier branching phyla, including Ctenophora and Porifera (Fig. 4) (74). As copulation evolved in multiple lineages, this molecular mechanism was either lost (i.e., Nematoda) or it took on new roles, such as the sAC-dependent sperm maturation process in mammals (i.e., capacitation) (Fig. 4) (30). Characterizing the evolution of this pathway will allow us to better understand both the shared and divergent traits underlying male fertility in metazoans.

Conclusion. Sexual reproduction is essential for the population growth, evolution, dispersal, and community dynamics of marine invertebrates (75). While climate change has impaired sexual reproduction across many marine taxa (76), the mechanisms driving these declines remain poorly understood. Ocean warming and acidification, two of the main climate change stressors affecting the ocean, may threaten sperm motility mechanisms that depend on precise intracellular pH by causing cytosolic acidification that may be prohibitively costly to overcome, thus preventing the signaling cascade necessary for motility. Cytosolic acidification may be especially costly to counteract for sperm, which have low cytoplasmic volume, limited energetic resources, and a brief lifespan (68). This could be an important bottleneck for population fitness, as sperm activation and motility are vital for fertilization across metazoan phyla. Importantly, the response of sperm to ocean acidification is nuanced, as both positive and negative shifts in sperm performance have been observed at the level of the individual male in molluscs and echinoderms (77–80). This phenotypic diversity highlights the need to better understand the fundamental mechanisms that regulate sperm performance in order to

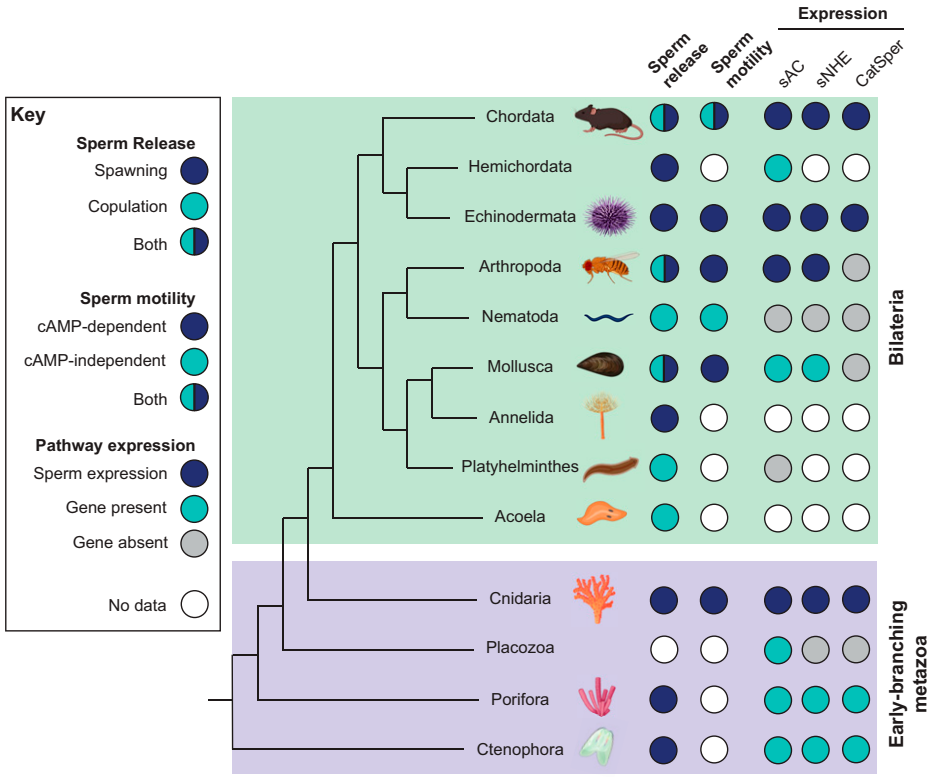

Fig. 4. Evolutionary conservation of the sperm motility activation pathway across Metazoan phyla. (*Left*) Sperm release strategies among the phyla. Spawning refers to release of sperm into an external aquatic environment for internal or external fertilization. Copulation refers to direct sperm transfer and internal fertilization. (*Middle*) Phyla in which one or more species exhibit cAMP-dependent sperm motility. (*Right*) Phyla in which one or more species have sAC, SLC9C1, or CatSper expression confirmed in sperm (blue), encoded in the genome (teal), or absent from all available genomes (gray). White circles indicate that no data were found in the published literature.

predict how the fitness of corals and other marine invertebrates will be affected by a changing marine environment.

Materials and Methods

Coral Sperm Intracellular pH and Motility Assays. Egg–sperm bundles were collected from *Montipora capitata* and allowed to break apart naturally in NaFSW (reference *SI Appendix, Supplemental Methods* for details). Sperm were loaded with 10 μM SNARF-1-AM for 15 min in the dark at room temperature, and fluorescence was imaged using a confocal microscope with 561 nm excitation and dual emission (585 and 640 ± 10 nm) at 25 °C. Sperm were imaged before and after addition of 20 mM NH_4Cl every 20 to 40 s over the next 7 min, and at least 14 cells and up to 149 cells were analyzed per time point. Sperm pH_i was calculated from the ratio (R) of SNARF1 fluorescence and an in vivo calibration curve generated as previously described (81). A binary (motile versus nonmotile) motility score was also quantified from the fluorescence images, as nonmotile sperm appeared round with smooth edges (*SI Appendix*, Fig. S1*A*), whereas motile sperm had an oblong shape with an irregular border (*SI Appendix*, Fig. S1*B*). Sperm motility was also quantified following inhibition of sAC with 50 μM KH7 relative to DMSO controls using phase contrast microscopy of 1) sperm in seawater, 2) sperm in NaFSW, and 3) sperm in NaFSW immediately following stimulation with NH_4Cl.

Production of cAMP Following Activation of Motility. Coral sperm suspended in NaFSW were treated with either 20 mM NH_4Cl or 0.1% DMSO control, and cAMP production was stopped with the addition of HCl (0.17 N final concentration) at 0, 5, 30, 60, 120, and 500 s postexposure. Sperm were lysed by sonication, and cAMP content was quantified by enzyme-linked immunosorbent assay and normalized to total protein.

Sequence Analyses. The presence of key components of the sperm motility activation pathway (sAC, PKA, SLC9C1, CatSper, GC-A, CNGK, and HCN) in corals was investigated by querying two *M. capitata* genomes (40, 47) using echinoderm or cnidarian homologs (reference *SI Appendix, Supplemental Methods* for more details). Each predicted gene coding sequence was then used as a query in a tBLASTn algorithm search of a sperm-specific RNA-seq database from *M. capitata* sperm (48). In silico comparisons of protein structure were carried out using the Clustal Omega multiple sequence alignment tool (82), prediction of transmembrane segments using the TMHMM server (83), and prediction of coiled-coil domains using the DeepCoil server (52).

Protein Expression. Sperm total protein was extracted, and protein expression of *mc*sAC and *mc*PKA were detected by Western blotting using custom anti-coral sAC antibodies (37) and commercial anti-PKA antibodies (Cell Signaling 4782), respectively. To detect phosphorylated PKA substrates, sperm in NaFSW were stimulated with 20 mM NH_4Cl and flash frozen after 0, 30, 60, or 120 s poststimulation and subjected to Western blotting with a phospho-PKA substrate antibody (RRXS*/T*; Cell Signaling 9642). Subcellular localization of *mc*sAC was determined by immunocytochemistry. Freshly collected sperm were fixed in 4% paraformaldehyde for 60 min at 4 °C, permeabilized in 0.3% Triton-X in phosphate-buffered saline for 3 min, and incubated with primary antibodies overnight at 4 °C. Cells were incubated with secondary antibodies for 1 h at room temperature in the dark, stained with NucBlue to label nuclei, and imaged using confocal microscopy.

Phylogenetic Analysis of pH-sAC-cAMP Signaling within Metazoa. A comparison of the reproductive strategies, sperm motility mechanisms, and sAC/sNHE/CatSper gene conservation was carried out through a search of the literature. Sources used in the compilation of the phylogenetic tree in Fig. 4 are described in *SI Appendix*, Fig. S5. All gene expression data were derived from ref. 74.

Data Availability. All study data are accessible as they are included in the article and/or supporting information.

ACKNOWLEDGMENTS. We thank Crawford Drury, Hollie Putnam, Ariana Huffmyer, and the staff at the Hawaii Institute of Marine Biology for logistical support during coral spawning and Martin Tresguerres for sharing coral sAC antibodies. The monoclonal antibodies, JLA-20 and E7, developed by the

University of Iowa and the University of Colorado at Boulder, respectively, were obtained from the Developmental Studies Hybridoma Bank, created by the National Institute of Child Health and Human Development of the NIH and maintained at The University of Iowa, Department of Biology, Iowa City, IA. Sperm were collected under Special Activity Permits 2020-41 and 2021-41.

All cartoons were created using BioRender.com and licensed for publication. This work was supported by the NSF Postdoctoral Research Fellowship in Biology 1812191 to K.F.S., NIH T32 Predoctoral Training Grant in Cell and Molecular Biology GM-07229 to L.A.-W., NSF-OCE 1923743 to K.L.B., and the Charles E. Kaufman Foundation New Investigator Award to K.L.B.

1. D. R. Levitan, C. Petersen, Sperm limitation in the sea. *Trends Ecol. Evol.* **10**, 228–231 (1995).
2. U. B. Kaupp, N. D. Kashikar, I. Weyand, Mechanisms of sperm chemotaxis. *Annu. Rev. Physiol.* **70**, 93–117 (2008).
3. C. R. Ward, G. S. Kopf, Molecular events mediating sperm activation. *Dev. Biol.* **158**, 9–34 (1993).
4. M. Q. Martindale, The evolution of metazoan axial properties. *Nat. Rev. Genet.* **6**, 917–927 (2005).
5. N. Knowlton *et al.*, "Coral reef biodiversity" in *Life in the World's Oceans: Diversity, Distribution, and Abundance*, A. McIntyre, Ed. (John Wiley and Sons, 2010), pp. 65–77.
6. N. Knowlton, The future of coral reefs. *Proc. Natl. Acad. Sci. U.S.A.* **98**, 5419–5425 (2001).
7. P. Kaniewska, S. Alon, S. Karako-Lampert, O. Hoegh-Guldberg, O. Levy, Signaling cascades and the importance of moonlight in coral broadcast mass spawning. *eLife* **4**, e09991 (2015).
8. O. Levy *et al.*, Light-responsive cryptochromes from a simple multicellular animal, the coral Acropora millepora. *Science* **318**, 467–470 (2007).
9. R. H. Richmond, K. H. Tisthammer, N. P. Spies, The effects of anthropogenic stressors on reproduction and recruitment of corals and reef organisms. *Front. Mar. Sci.* **5**, 226 (2018).
10. M. Hagedorn *et al.*, Potential bleaching effects on coral reproduction. *Reprod. Fertil. Dev.* **28**, 1061–1071 (2016).
11. D. R. Levitan, W. Boudreau, J. Jara, N. Knowlton, Long-term reduced spawning in *Orbicella* coral species due to temperature stress. *Mar. Ecol. Prog. Ser.* **515**, 1–10 (2014).
12. O. Hoegh-Guldberg, E. S. Poloczanska, W. Skirving, S. Dove, Coral reef ecosystems under climate change and ocean acidification. *Front. Mar. Sci.* **4**, 158 (2017).
13. M. Byrne, "Impact of ocean warming and ocean acidification on marine invertebrate life history stages: Vulnerabilities and potential for persistance in a changing ocean" in *Oceanography and Marine Biology: An Annual Review*, R. N. Gibson, R. J. A. Atkinson, J. D. M. Gordon, Eds. (CRC Press, 2011), pp. 1–42.
14. J. Fisch, C. Drury, E. K. Towle, R. N. Winter, M. W. Miller, Physiological and reproductive repercussions of consecutive summer bleaching events of the threatened Caribbean coral Orbicella faveolata. *Coral Reefs* **38**, 863–876 (2019).
15. M. Morita *et al.*, Ocean acidification reduces sperm flagellar motility in broadcast spawning reef invertebrates. *Zygote* **18**, 103–107 (2010).
16. M. Nakamura, M. Morita, Sperm motility of the scleractinian coral Acropora digitifera under preindustrial, current, and predicted ocean acidification regimes. *Aquat. Biol.* **15**, 299–302 (2012).
17. R. Albright, B. Mason, Projected near-future levels of temperature and pCO_2 reduce coral fertilization success. *PLoS One* **8**, e56468 (2013).
18. R. Albright, B. Mason, M. Miller, C. Langdon, Ocean acidification compromises recruitment success of the threatened Caribbean coral Acropora palmata. *Proc. Natl. Acad. Sci. U.S.A.* **107**, 20400–20404 (2010).
19. T. Innis *et al.*, Marine heatwaves depress metabolic activity and impair cellular acid-base homeostasis in reef-building corals regardless of bleaching susceptibility. *Glob. Change Biol.* **27**, 2728–2743 (2021).
20. E. M. Gibbin, H. M. Putnam, S. K. Davy, R. D. Gates, Intracellular pH and its response to CO2-driven seawater acidification in symbiotic versus non-symbiotic coral cells. *J. Exp. Biol.* **217**, 1963–1969 (2014).
21. M. C. Esposito, R. Boni, A. Cuccaro, E. Tosti, A. Gallo, Sperm motility impairment in free spawning invertebrates under near-future level of ocean acidification: Uncovering the mechanism. *Front. Mar. Sci.* **6**, 794 (2020).
22. R. Christen, R. W. Schackmann, B. M. Shapiro, Metabolism of sea urchin sperm. Interrelationships between intracellular pH, ATPase activity, and mitochondrial respiration. *J. Biol. Chem.* **258**, 5392–5399 (1983).
23. M. Morita *et al.*, Eggs regulate sperm flagellar motility initiation, chemotaxis and inhibition in the coral Acropora digitifera, A. gemmifera and A. tenuis. *J. Exp. Biol.* **209**, 4574–4579 (2006).
24. R. Christen, R. W. Schackmann, B. M. Shapiro, Elevation of the intracellular pH activates respiration and motility of sperm of the sea urchin, Strongylocentrotus purpuratus. *J. Biol. Chem.* **257**, 14881–14890 (1982).
25. A. Nakajima, M. Morita, A. Takemura, S. Kamimura, M. Okuno, Increase in intracellular pH induces phosphorylation of axonemal proteins for activation of flagellar motility in starfish sperm. *J. Exp. Biol.* **208**, 4411–4418 (2005).
26. F. Windler *et al.*, The solute carrier SLC9C1 is a Na^+/H^+-exchanger gated by an S4-type voltage-sensor and cyclic-nucleotide binding. *Nat. Commun.* **9**, 2809 (2018).
27. V. D. Vacquier, A. Loza-Huerta, J. García-Rincón, A. Darszon, C. Beltrán, Soluble adenylyl cyclase of sea urchin spermatozoa. *Biochim. Biophys. Acta* **1842**, 2621–2628 (2014).
28. M. Morita, A. Iguchi, A. Takemura, Roles of calmodulin and calcium/calmodulin-dependent protein kinase in flagellar motility regulation in the coral Acropora digitifera. *Mar. Biotechnol. (NY)* **11**, 118–123 (2009).
29. Y. Zhang *et al.*, Discovery of a receptor guanylate cyclase expressed in the sperm flagella of stony corals. *Sci. Rep.* **9**, 14652 (2019).
30. K. C. Hess *et al.*, The "soluble" adenylyl cyclase in sperm mediates multiple signaling events required for fertilization. *Dev. Cell* **9**, 249–259 (2005).
31. D. Wang, S. M. King, T. A. Quill, L. K. Doolittle, D. L. Garbers, A new sperm-specific Na+/H+ exchanger required for sperm motility and fertility. *Nat. Cell Biol.* **5**, 1117–1122 (2003).
32. F. Xie *et al.*, Soluble adenylyl cyclase (sAC) is indispensable for sperm function and fertilization. *Dev. Biol.* **296**, 353–362 (2006).
33. G. Esposito *et al.*, Mice deficient for soluble adenylyl cyclase are infertile because of a severe sperm-motility defect. *Proc. Natl. Acad. Sci. U.S.A.* **101**, 2993–2998 (2004).
34. D. Ren *et al.*, A sperm ion channel required for sperm motility and male fertility. *Nature* **413**, 603–609 (2001).
35. M. A. Nolan *et al.*, Sperm-specific protein kinase A catalytic subunit Calpha2 orchestrates cAMP signaling for male fertility. *Proc. Natl. Acad. Sci. U.S.A.* **101**, 13483–13488 (2004).
36. K. L. Barott *et al.*, High adenylyl cyclase activity and in vivo cAMP fluctuations in corals suggest central physiological role. *Sci. Rep.* **3**, 1379 (2013).
37. K. L. Barott, M. E. Barron, M. Tresguerres, Identification of a molecular pH sensor in coral. *Proc. Biol. Sci.* **284**, 20171769 (2017).
38. H. C. Lee, C. Johnson, D. Epel, Changes in internal pH associated with initiation of motility and acrosome reaction of sea urchin sperm. *Dev. Biol.* **95**, 31–45 (1983).
39. P. Y. Wong, W. M. Lee, A. Y. Tsang, The effects of extracellular sodium on acid release and motility initiation in rat caudal epididymal spermatozoa in vitro. *Exp. Cell Res.* **131**, 97–104 (1981).
40. A. Shumaker *et al.*, Genome analysis of the rice coral Montipora capitata. *Sci. Rep.* **9**, 2571 (2019).
41. Y. Chen *et al.*, Soluble adenylyl cyclase as an evolutionarily conserved bicarbonate sensor. *Science* **289**, 625–628 (2000).
42. S. Kleinboelting *et al.*, Crystal structures of human soluble adenylyl cyclase reveal mechanisms of catalysis and of its activation through bicarbonate. *Proc. Natl. Acad. Sci. U.S.A.* **111**, 3727–3732 (2014).
43. J. Buck, M. L. Sinclair, L. Schapal, M. J. Cann, L. R. Levin, Cytosolic adenylyl cyclase defines a unique signaling molecule in mammals. *Proc. Natl. Acad. Sci. U.S.A.* **96**, 79–84 (1999).
44. J. A. Chaloupka, S. A. Bullock, V. Iourgenko, L. R. Levin, J. Buck, Autoinhibitory regulation of soluble adenylyl cyclase. *Mol. Reprod. Dev.* **73**, 361–368 (2006).
45. J. Farrell *et al.*, Somatic 'soluble' adenylyl cyclase isoforms are unaffected in $Sacy^{tm1\text{-}Lex}$/$Sacy^{tm1Lex}$ 'knockout' mice. *PLoS One* **3**, e3251 (2008).
46. J. L. Padilla-Gamiño, T. M. Weatherby, R. G. Waller, R. D. Gates, Formation and structural organization of the egg–sperm bundle of the scleractinian coral Montipora capitata. *Coral Reefs* **30**, 371–380 (2011).
47. M. Helmkampf, M. R. Bellinger, S. M. Geib, S. B. Sim, M. Takabayashi, Draft genome of the rice coral Montipora capitata obtained from linked-read sequencing. *Genome Biol. Evol.* **11**, 2045–2054 (2019).
48. J. Van Etten, A. Shumaker, T. Mass, H. M. Putnam, D. Bhattacharya, Transcriptome analysis provides a blueprint of coral egg and sperm functions. *PeerJ* **8**, e9739 (2020).
49. M. J. Moore, J. R. Kanter, K. C. Jones, S. S. Taylor, Phosphorylation of the catalytic subunit of protein kinase A. Autophosphorylation versus phosphorylation by phosphoinositide-dependent kinase-1. *J. Biol. Chem.* **277**, 47878–47884 (2002).
50. S. K. Aggarwal, R. MacKinnon, Contribution of the S4 segment to gating charge in the Shaker K+ channel. *Neuron* **16**, 1169–1177 (1996).
51. B. Navarro, Y. Kirichok, J.-J. Chung, D. E. Clapham, Ion channels that control fertility in mammalian spermatozoa. *Int. J. Dev. Biol.* **52**, 607–613 (2008).
52. J. Ludwiczak, A. Winski, K. Szczepaniak, V. Alva, S. Dunin-Horkawicz, DeepCoil-a fast and accurate prediction of coiled-coil domains in protein sequences. *Bioinformatics* **35**, 2790–2795 (2019).
53. H. Qi *et al.*, All four CatSper ion channel proteins are required for male fertility and sperm cell hyperactivated motility. *Proc. Natl. Acad. Sci. U.S.A.* **104**, 1219–1223 (2007).
54. Z. M. James, W. N. Zagotta, Structural insights into the mechanisms of CNBD channel function. *J. Gen. Physiol.* **150**, 225–244 (2018).
55. P. Labarca *et al.*, A cAMP regulated K+-selective channel from the sea urchin sperm plasma membrane. *Dev. Biol.* **174**, 271–280 (1996).
56. R. Gauss, R. Seifert, U. B. Kaupp, Molecular identification of a hyperpolarization-activated channel in sea urchin sperm. *Nature* **393**, 583–587 (1998).
57. B. H. Gibbons, I. R. Gibbons, Flagellar movement and adenosine triphosphatase activity in sea urchin sperm extracted with triton X-100. *J. Cell Biol.* **54**, 75–97 (1972).
58. M. A. Battistone *et al.*, Functional human sperm capacitation requires both bicarbonate-dependent PKA activation and down-regulation of Ser/Thr phosphatases by Src family kinases. *Mol. Hum. Reprod.* **19**, 570–580 (2013).
59. U. B. Kaupp *et al.*, The signal flow and motor response controling chemotaxis of sea urchin sperm. *Nat. Cell Biol.* **5**, 109–117 (2003).

60. M. G. Buffone, E. V. Wertheimer, P. E. Visconti, D. Krapf, Central role of soluble adenylyl cyclase and cAMP in sperm physiology. *Biochim. Biophys. Acta* **1842**, 2610–2620 (2014).
61. S. Mukherjee *et al.*, A novel biosensor to study cAMP dynamics in cilia and flagella. *eLife* **5**, e14052 (2016).
62. C. Brenker *et al.*, The CatSper channel: A polymodal chemosensor in human sperm. *EMBO J.* **31**, 1654–1665 (2012).
63. D. Wang *et al.*, A sperm-specific Na+/H+ exchanger (sNHE) is critical for expression and in vivo bicarbonate regulation of the soluble adenylyl cyclase (sAC). *Proc. Natl. Acad. Sci. U.S.A.* **104**, 9325–9330 (2007).
64. C. Beltrán *et al.*, Particulate and soluble adenylyl cyclases participate in the sperm acrosome reaction. *Biochem. Biophys. Res. Commun.* **358**, 1128–1135 (2007).
65. F. Valsecchi, L. S. Ramos-Espiritu, J. Buck, L. R. Levin, G. Manfredi, cAMP and mitochondria. *Physiology (Bethesda)* **28**, 199–209 (2013).
66. A. Loza-Huerta, R. Vera-Estrella, A. Darszon, C. Beltrán, Certain Strongylocentrotus purpuratus sperm mitochondrial proteins co-purify with low density detergent-insoluble membranes and are PKA or PKC-substrates possibly involved in sperm motility regulation. *Biochim. Biophys. Acta* **1830**, 5305–5315 (2013).
67. P. Schlegel, M. T. Binet, J. N. Havenhand, C. J. Doyle, J. E. Williamson, Ocean acidification impacts on sperm mitochondrial membrane potential bring sperm swimming behaviour near its tipping point. *J. Exp. Biol.* **218**, 1084–1090 (2015).
68. V. Bondarenko, J. Cosson, Structure and beating behavior of the sperm motility apparatus in aquatic animals. *Theriogenology* **135**, 152–163 (2019).
69. W. Bönigk *et al.*, An atypical CNG channel activated by a single cGMP molecule controls sperm chemotaxis. *Sci. Signal.* **2**, ra68 (2009).
70. R. Seifert *et al.*, The CatSper channel controls chemosensation in sea urchin sperm. *EMBO J.* **34**, 379–392 (2015).
71. B. S. Jaiswal, M. Conti, Identification and functional analysis of splice variants of the germ cell soluble adenylyl cyclase. *J. Biol. Chem.* **276**, 31698–31708 (2001).
72. M. Yoshida, J. F. Asturiano, *Reproduction in Aquatic Animals: From Basic Biology to Aquaculture Technology* (Springer Nature, 2020).
73. M. Boulais, M. Demoy-Schneider, S. M. H. Alavi, J. Cosson, Spermatozoa motility in bivalves: Signaling, flagellar beating behavior, and energetics. *Theriogenology* **136**, 15–27 (2019).
74. F. Romero, T. Nishigaki, Comparative genomic analysis suggests that the sperm-specific sodium/proton exchanger and soluble adenylyl cyclase are key regulators of CatSper among the Metazoa. *Zoological Lett.* **5**, 25 (2019).
75. J. P. Crimaldi, R. K. Zimmer, The physics of broadcast spawning in benthic invertebrates. *Annu. Rev. Mar. Sci.* **6**, 141–165 (2014).
76. K. J. Kroeker, R. L. Kordas, R. N. Crim, G. G. Singh, Meta-analysis reveals negative yet variable effects of ocean acidification on marine organisms. *Ecol. Lett.* **13**, 1419–1434 (2010).
77. J. N. Havenhand, P. Schlegel, Near-future levels of ocean acidification do not affect sperm motility and fertilization kinetics in the oyster Crassostrea gigas. *Biogeosciences* **6**, 3009–3015 (2009).
78. R. A. Lymbery, W. J. Kennington, C. E. Cornwall, J. P. Evans, Ocean acidification during prefertilization chemical communication affects sperm success. *Ecol. Evol.* **9**, 12302–12310 (2019).
79. K. E. Smith *et al.*, Sea urchin reproductive performance in a changing ocean: Poor males improve while good males worsen in response to ocean acidification. *Proc. Biol. Sci.* **286**, 20190785 (2019).
80. A. L. Campbell, D. R. Levitan, D. J. Hosken, C. Lewis, Ocean acidification changes the male fitness landscape. *Sci. Rep.* **6**, 31250 (2016).
81. A. A. Venn *et al.*, Imaging intracellular pH in a reef coral and symbiotic anemone. *Proc. Natl. Acad. Sci. U.S.A.* **106**, 16574–16579 (2009).
82. F. Sievers *et al.*, Fast, scalable generation of high-quality protein multiple sequence alignments using Clustal Omega. *Mol. Syst. Biol.* **7**, 539 (2011).
83. E. L. Sonnhammer, G. von Heijne, A. Krogh, A hidden Markov model for predicting transmembrane helices in protein sequences. *Proc. Int. Conf. Intell. Syst. Mol. Biol.* **6**, 175–182 (1998).